Separation and Purification Technology 374 (2025) 133712

Contents lists available at ScienceDirect

Separation and Purification Technology

journal homepage: www.elsevier.com/locate/seppur

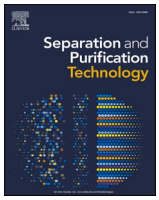

Sustainable leaching of metals from waste printed circuit boards using efficient carboxylic acid-based deep eutectic solvents

Emmanuel Anuoluwapo Oke *, Johannes Hermanus Potgieter

Sustainable and Innovative Minerals and Metals Extraction Technology (SIMMET) Research Group, School of Chemical and Metallurgical Engineering, University of the Witwatersrand, Private Bag X3 PO Wits 2050, Johannesburg, South Africa

ARTICLE INFO

Editor: Dr. B. Van der Bruggen

Keywords:
E-waste
Resource recovery
Waste management
Shrinking core model
Activation energy

ABSTRACT

The exponential growth in electronic waste presents a substantial environmental and economic challenge due to its high content of valuable metals. So, in this study, we investigated the use of carboxylic acid-based deep eutectic solvents (DESs) for the leaching of base metals (Cu, Al, Fe, Sn, and Sc) from waste printed circuit boards (WPCBs). The DESs used were prepared at a 1:2 M ratio from choline chloride (ChCl) used as hydrogen bond acceptor (HBA) with either chloroacetic acid (CAA), dichloroacetic acid (DCA), or trichloroacetic acid (TCA) as hydrogen bond donors (HBDs). The influence of the DES type on the leaching of the metals studied follows the order: ChCl:TCA > ChCl:DCA > ChCl:CAA. Specifically, ChCl:TCA DES displayed the best leaching efficiencies by achieving leaching efficiencies of 87.3 % for Cu, 85.3 % for Al, 89.9 % for Fe, 68.4 % for Sn, and 60.6 % for Sc at a temperature of 45 °C and contact time of 3.0 h in the presence of 1.0 M H_2O_2 with the grain size of 212 μm under 500 rpm agitation and solid-to-liquid ratio of 1:10. Outstanding leaching efficiencies of 100.0 %, 98.5 %, 95.3 %, 91.9 %, and 82.6 % were obtained for Cu, Al, Fe, Sn, and Sc respectively when the temperature was raised to 65 °C and the grain size reduced to 106 μm. Furthermore, kinetic analysis involving both diffusion- and chemical reaction-controlled models, yielded activation energies below 40.0 $kJmol^{-1}$ for all metals, suggesting a diffusion-controlled leaching mechanism.

1. Introduction

The fastest-growing waste stream worldwide is believed to be electronic waste, or "e-waste," which has recently gained attention globally. An annual growth rate of more than 70 million tonnes is projected for e-waste [1]. Approximately 4–7 % of the mass of all e-waste is made up of waste-printed circuit boards (WPCBs) [2]. It is further estimated that global e-waste production will surpass 120 million tonnes by 2050, presenting increased challenges for e-waste disposal [3]. Although e-waste represents an economic opportunity, with an estimated annual value of 91 billion US dollars, it is reported that only 22.3 % of this waste is formally recycled each year [4]. Metals including Au, Cu, Ag, Zn, Al, and Pb, among others, are present in WPCBs along with polymers, ceramics, and other materials [5]. Consequently, the secret to modern recycling is the resource recovery of metals from WPCBs using an effective and environmentally friendly technique. Thus, modern recycling depends on the resource recovery of metals from WPCBs using an effective and environmentally friendly process. Only a few of the 60 chemical elements (8–12) are presently being researched for strategic recycling [6,7]. Today, there is a greater demand for metals, and recycling is a crucial component of metal sustainability. Many metals, including Cu, Zn, Ni, Al, Fe, Pb, and Sn (base metals), as well as precious metals like Au, Ag, Pd, and Pt, and rare earth metals like Y, Eu, Ce, Gd, and La, can be found in the e-waste produced worldwide [6,8]. Notably, the United Nations strongly promotes e-waste recycling, making it a top priority under the Sustainable Development Goals [9].

In response to the long-term demand for metals, Watari et al. examined the anticipated global requirements for key metals commonly extracted from large mines, including Fe, Al, Cu, Zn, Pb, and Ni, as projected for 2030 and 2050 [10]. They predict that by 2050, the growth rates for these metals will be 215.0 % for Al, 140.0 % for Cu, 140.0 % for Ni, 86.0 % for Fe, 81.0 % for Zn, and 46.0 % for Pb, compared to 2010 levels. Additionally, by the century's end, demand for most major metals (excluding Pb) is expected to rise significantly, with Al seeing growth of 470.0 %, Cu 330.0 %, Zn 130.0 %, and Fe 100.0 %. Schipper et al. further estimated that the demand for Cu alone could reach approximately 120 million tonnes by 2050, based on regression analysis [11]. This urgent situation imposes substantial pressure on metal mineral

* Corresponding author.
E-mail addresses: emmanuel.oke@wits.ac.za, okeemmanuela@gmail.com (E.A. Oke).

https://doi.org/10.1016/j.seppur.2025.133712
Received 28 March 2025; Received in revised form 6 May 2025; Accepted 23 May 2025
Available online 23 May 2025

resources, making it a significant global challenge to satisfy the increasing demand for metals necessary for the advancement of human society.

The widely recognised hydrometallurgical, pyrometallurgical and biometallurgical processes are the most commonly used techniques for recycling metals from WPCBs [12]. In pyrometallurgy, metal and non-metal components are separated at high temperatures using variations in melting and boiling points between the constituents of e-waste [13,14]. Through pyrolysis at 330 °C, Chen et al. were able to recover 92.0 % Cu and 99.8 % Sn from the WPCBs in the form of Cu^0 and Cu-Sn alloys, respectively [15]. Variations in the grades of Cu recovered from the pyrolysis of WPCBs, conducted under varying temperatures, atmospheres, and durations, were revealed by the research of Faraji et al. [16]. It is critical to recognise that integrating complementary technologies is usually necessary for base metal separation. Jadhao et al. employed a low-temperature pyrolysis technique in conjunction with ultrasonic treatment to achieve the recovery of approximately 90.0 % of the metals by separating the pyrolysed solid residue through ultrasonic methods, conducted at 400 °C [17]. However, the drawbacks of pyrometallurgy for recovering metals from WPCBs include high energy consumption, the release of toxic emissions, and the potential loss of valuable metals due to incomplete recovery.

Biometallurgy differs from pyrometallurgy in that it utilises the action of microorganisms to transform metals in e-waste from an insoluble to a soluble state, thus providing raw materials for further purification. This process can be categorised into bioleaching and bioadsorption [18]. Bioleaching involves converting precious metals in e-waste from a solid phase to a liquid phase through microbial metabolism, while bioadsorption uses specific media within microorganisms to facilitate ion exchange or complex reactions with metals [19]. Kaur et al. assessed the biosorption and bioleaching capabilities of seven microbial cultures using WPCBs as substrates, with *Pleurotus florida* and *Pseudomonas* spp. demonstrating the highest and distinct capacities for the biosorption and bioleaching of Cu and Fe, attributed to the bio-catalytic activity of laccase enzymes [18]. *Acidithiobacillus ferrooxidans* is commonly utilised in the bioleaching process of Cu [20]. The reaction mechanism involves the oxidation of Fe^{2+} to Fe^{3+}, which then oxidises Cu to Cu^{2+}. The resulting ferrous ions are continuously re-oxidised, enabling the ongoing leaching of Cu. Cu was recovered from WPCBs using bio-ferric sulfate, and waste Fe^{3+} can be replenished in a flooded bed without lowering redox potential as a result of Fe^{3+} consumption [21]. After 25 days of leaching, the recovery of Cu increased from 62.2 % to 90.0 %, significantly increasing the rate of Cu dissolution. Arslan recovered Cu, Ni, Zn, and Al from WPCBs using a mixed culture of *A. ferrooxidans* and *A. thiooxidans* that had been adapted to work with WPCBs [22]. After 10 days of leaching under ideal conditions, the recoveries of Cu, Ni, Zn, and Al were 94.0 %, 89.0 %, 88.0 %, and 59.0 %, respectively. The drawbacks of biometallurgy in recovering metals from WPCBs are slow processing times, limited efficiency with some metals, and the need for specific environmental conditions to support microbial activity.

Common hydrometallurgical processes for WPCBs involve pre-treatment, selective leaching of metals, purification of the leachate, and the recovery of metals as final products [23]. Chemical leaching methods, including inorganic acids and ammonia-ammonium solutions, are frequently used to recover base metals. Studies have shown that inorganic acids can efficiently leach different base metals from WPCBs under relatively mild conditions [24]. NH_3/NH_4^+ solutions can leach Cu selectively by forming stabilised $[Cu(NH_3)^{2+}]$ complexes [25]. However, the consumption of leaching agents has posed challenges for researchers and impeded the industrialisation of these technologies. Additionally, the slow leaching rate prolongs the time required to obtain a metal-rich solution, making the process inherently time-consuming. To improve the efficiency of base metal leaching processes, oxidising agents such as H_2O_2, I_2, $K_2Cr_2O_7$, $KMnO_4$, Cu^{2+}, and Fe^{3+} are often added [12]. Jadhao et al. demonstrated that an ammonia-ammonium solution with 0.4 M H_2O_2 can extract 100.0 % Cu and 90.0 % Ni from WPCBs [26]. Research has focused on enhancing leaching rates using better lixiviants and electrochemical methods. Xia et al. used ceric ammonium nitrate for Cu dissolution, with recovery through diaphragm electrolysis [27]. Selective leaching of metals can be achieved by adjusting reagent ratios, while subsequent processing can recover Zn and Sn. However, using ammonia-ammonium solutions and inorganic acids poses safety risks due to their corrosive and volatile nature, particularly at high temperatures, and may lead to secondary environmental contamination. Owing to the highlighted disadvantages of the existing methods, it is imperative to develop faster and more environmentally benign techniques. In this case, the use of deep eutectic solvents (DESs) for leaching metals from WPCBs could be one of the possible ways forward.

With its low melting point, broad electrochemical window, high conductivity, unique solubility for metal oxides, inexpensive nature, and easy preparation, DESs are eco-friendly solvents [28]. The synthesis of DESs using different carboxylic acids as hydrogen bond donors (HBDs) and choline chloride (ChCl) as a hydrogen bond acceptor (HBA) was published by Abbot et al. in 2004 [29]. This method demonstrated effective solvation of metal oxides and has potential uses in metal extraction. Because of their particular stoichiometric ratio of HBAs and HBDs, DESs have a lower melting point than their constituent parts. Internal interactions are responsible for creating a highly asymmetric structure and lowering lattice energy [30]. From a green chemistry perspective, DESs generally demonstrate lower toxicity and improved biodegradability due to the natural origins of their precursors [31]. Additionally, DESs utilise readily available and inexpensive raw materials, enabling straightforward mixing of components with 100.0 % atom economy and eliminating the need for further purification [32]. Due to these unique properties of DESs, Cu, Al, Fe, Sc and Sn were leached from WPCB of desktop computers using DESs composed of ChCl (HBA) and various HBDs, including chloroacetic acid (CAA), dichloroacetic acid (DCA) and trichloroacetic acid (TCA). ChCl was chosen as HBA in DESs preparation due to its strong hydrogen bonding ability, low toxicity, biodegradability, and affordability. CAA, DCA and TCA were selected as HBDs for their varying acid strengths and electron-withdrawing properties. To the best of the authors' knowledge, these DESs have not been reported in the literature for the leaching of metals from WPCBs before. Through the use of these DESs, this study aims to contribute to the growing literature on metal leaching with DESs and to suggest viable and efficient processes for the recovery of selected metals from WPCBs.

2. Experimental

2.1. Chemicals

Choline chloride (ChCl) was purchased from Sigma Aldrich with a purity of $\geq$ 99.0 %. Chloroacetic acid (CAA) was sourced from Associated Chemical Enterprises Pty Ltd, with a purity of $\geq$ 99.0 %, while dichloroacetic acid (DCA) and trichloroacetic acid (TCA) were obtained from Sigma Aldrich with a purity of $\geq$ 99.0 %. Furthermore, 50.0 % hydrogen peroxide (H_2O_2) was acquired from Associated Chemical Enterprises Pty. All chemicals were used without further purification, and all solutes were dissolved in deionised water.

2.2. Collection and pre-treatment of WPCBs

For this study, 15 central processing units from HP desktop computers were collected from the School of Chemical and Metallurgical Engineering, University of the Witwatersrand, Johannesburg. The first step involved manually stripping the printed circuit boards (PCBs) using pliers and screwdrivers. After this stage, the stripped PCBs were further depopulated, and their weights before and after depopulation were measured using a weighing machine. Detailed information about the computers and PCBs is available in the supplementary information (**Table S1**). The depopulated PCBs were then cut into smaller pieces and

soaked in 5.0 M NaOH to remove the resin and organic layers, thereby exposing the metals for more efficient recovery. Following this, the PCBs were thoroughly rinsed under running tap water until they reached the same pH as the tap water. The treated waste PCBs were then crushed multiple times and sieved into 106 μm, 212 μm, 300 μm, 400 μm, and 500 μm size fractions using an automatic sieve, as shown in Fig. 1. Finally, representative samples were selected from the crushed PCBs to determine the metal contents using X-ray fluorescence (XRF), with the results presented in Table 1. The variation in Al, Cu, and Fe concentrations across different grain sizes in PCBs is likely due to the differences in the distribution of these metals within the PCB material. Also, the morphology of the WPCBs was determined before and after leaching using scanning electron microscopy with energy-dispersive X-ray spectroscopy (SEM-EDX). Furthermore, the X-ray diffraction pattern was also examined from ground WPCBs before and after leaching using an X-ray diffractometer (XRD).

The results in Table 1 clearly indicates that Al, Fe and Sc are concentrated in the finest size fraction, while Cu and Sn are concentrated in the largest size fraction. Furthermore, although the concentration of scandium in waste PCBs is relatively low in absolute terms (0.085–0.154 wt% i.e. 850–1540 ppm), these values exceed the typical grades found in primary magmatic and supergene Sc deposits, many of which range from 40 to 300 ppm [33]. Therefore, the Sc concentrations observed in our PCB samples are significantly higher than those considered economically viable in primary deposits, particularly when Sc is recovered alongside more abundant base metals like Cu, Al, and Sn. Considering scandium's designation as a strategic metal, its high market value, and the limited number of reliable global suppliers, the recovery of Sc from PCBs could be a viable supplementary source. This is especially pertinent in the context of urban mining, where multiple valuable metals can be simultaneously recovered using environmentally benign solvents.

2.3. Preparation of carboxylic acid-based DESs

Three DESs were synthesised with ChCl as HBA and CAA, DCA and TCA as HBDs in a 1:2 M ratio, forming ChCl:CAA, ChCl:DCA, and ChCl:TCA DESs. These mixtures were stirred on a thermostatically controlled hot plate with a magnetic stirrer at 40.0 °C and 500.0 rpm until homogeneous solutions free of precipitates formed. The preparation process for the DESs is shown in Fig. 2. This method aligns with the procedure used by Ferrera et al. in their recent investigation on the stability of ChCl-based DESs involving carboxylic acids [34]. After synthesis, the DESs were placed in a desiccator to remove moisture and then stored in sealed glass vials to prevent any structural changes or environmental impact on their physical and chemical properties. No additional purification was necessary, and the DESs were characterised by Fourier-transform infrared (FT-IR) spectroscopy to examine their chemical structures.

Table 1
XRF results of the pre-leached WPCBs of different grain sizes.

Grain Size	Al (Mass %)	Fe (Mass %)	Cu (Mass %)	Sn (Mass %)	Sc (Mass %)
106 μm	28.50	18.70	6.85	5.41	0.154
212 μm	28.30	11.40	17.50	7.30	0.127
300 μm	17.30	7.24	36.10	8.61	0.132
400 μm	17.60	4.55	40.20	7.92	0.145
500 μm	18.00	2.86	46.80	8.98	0.085

2.4. Rheological behaviour of DESs

The rheological behaviour of the DESs was examined using an Anton Paar MCR 102 Modular Compact Rheometer, equipped with a CP 40 cone-plate measuring setup. The cone angle was set at 1°, with a 0.1 mm gap between the cone and plate. Temperature was regulated by a P-PTD 200/AIR Peltier device. Steady shear measurements were carried out at 298.15 K across a shear rate range of 1.0 to 100.0 s^{-1}.

2.5. Leaching procedure

A solid-to-liquid (S/L) ratio of 1:10 was applied in this investigation. The leaching experiment for the ground WPCB sample, both with and without the H_2O_2 oxidant, was conducted under atmospheric conditions in a 250.0 mL two-necked round-bottom flask. The flask was submerged in a water bath and placed on a thermostatically controlled hot plate with a magnetic stirrer. One neck of the flask, functioning as the leaching reactor, was attached to a water-cooled condenser, while the other held a thermometer immersed in the leaching solution. A stirring bar within the flask maintained uniform mixing at 500.0 rpm. Removal temperatures ranged from 25 °C to 65 °C, and reaction times varied from 1.0 to 5.0 h. The resulting solution was filtered using a 0.45 μm glass

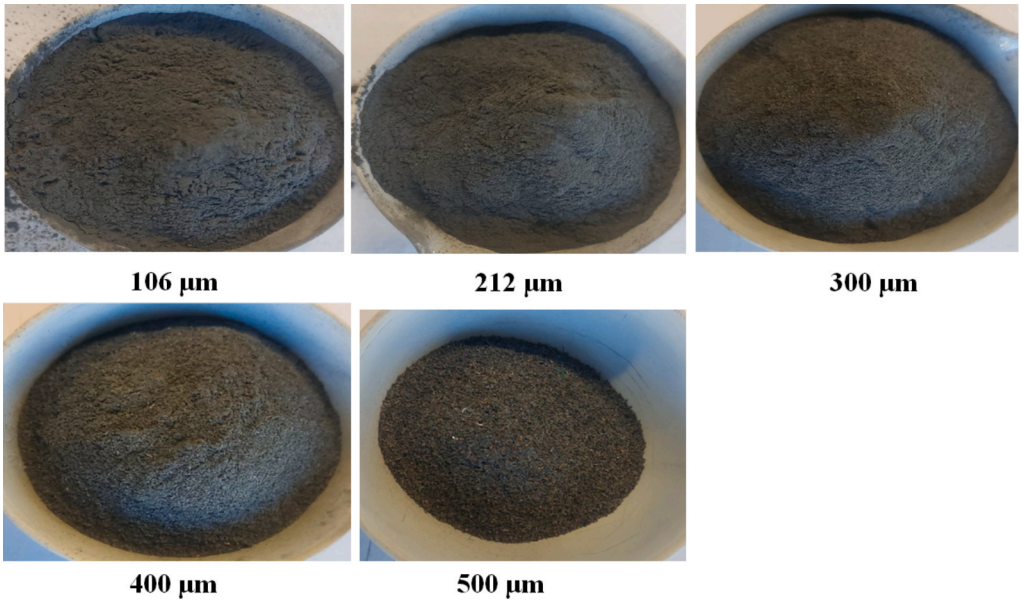

Fig. 1. Images of different grain sizes of WPCBs.

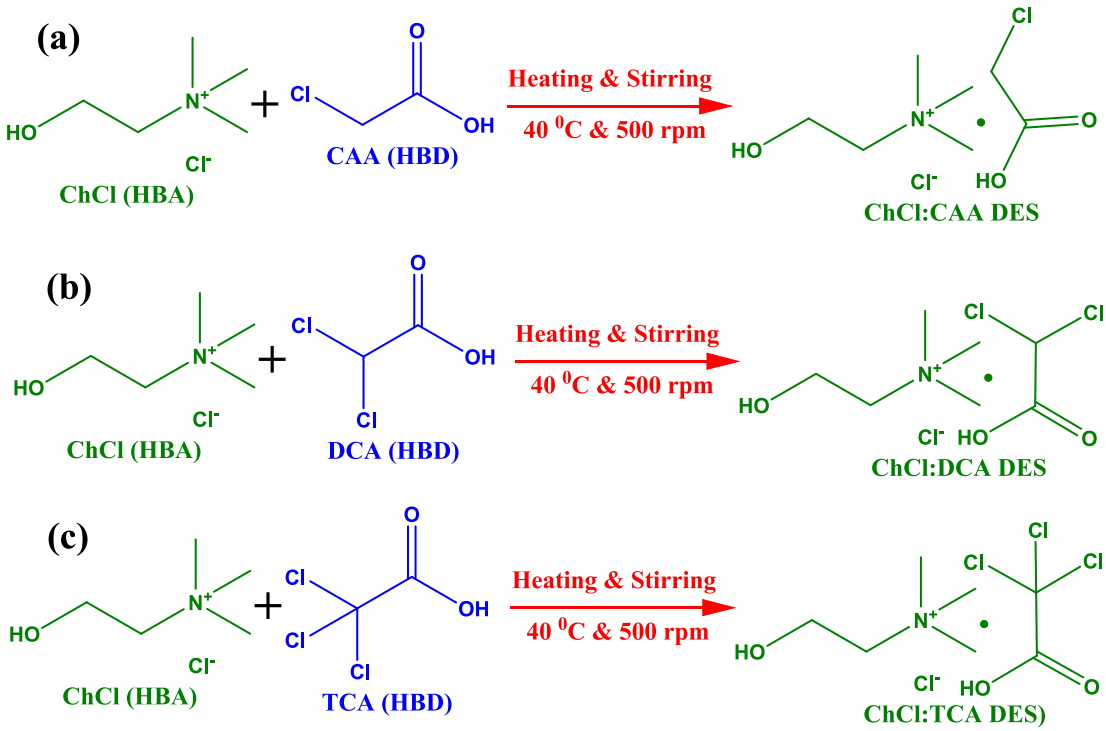

Fig. 2. Preparation of DESs used in this study.

fibre filter attached to a syringe and then diluted with deionised water prior to metal analysis by inductively coupled plasma optical emission spectrometry (ICP-OES). To minimise experimental error, each experiment was replicated two times under identical conditions, and results were subsequently averaged. During the experiment, leaching efficiency was calculated using equation (1).

$$\boldsymbol{LeachingEfficiency}(\%) = \frac{\boldsymbol{K} \times \boldsymbol{L}}{\boldsymbol{M} \times \boldsymbol{N}} \times 100 \quad (1)$$

In this case, *K* represents the concentration of target metal in the leached solution, *L* designates the volume of the leached solution, *M* denotes the amount of metal of interest within the original sample and *N* represents the weight of the sample.

3. Results and discussion

3.1. Dess FT-IR characterisation

The FTIR spectra analysis was conducted to investigate the interactions among the internal functional groups within the prepared DESs. The spectra for ChCl, CAA, DCA, TCA, and their corresponding DESs (ChCl:CAA, ChCl:DCA, and ChCl:TCA) are shown in **Fig. S1(a-c)**. In **Fig. S1(a)**, the peak observed around 3330 cm^{-1} corresponds to the − OH stretching vibration, characteristic of hydrogen bonding in ChCl. Additionally, the − CH_2 bending vibration for ChCl appears near 1481 cm^{-1}. For CAA, a significant peak around 1725 cm^{-1} is attributed to the − CO stretching vibration, indicative of the carboxylic acid group. The spectra for ChCl:CAA demonstrate shifts in these peaks, suggesting enhanced hydrogen bonding interactions between ChCl and CAA. In **Fig. S1(b)**, the FT-IR spectra for ChCl and DCA show a broad − OH stretching band around 3330 cm^{-1} in ChCl and a distinctive − CO stretching peak at approximately 1717 cm^{-1} for DCA. When ChCl and DCA are combined to form the DES (ChCl:DCA), a slight blue shift in the − OH stretching vibration is observed, implying stronger hydrogen bonding between the two components. Also, in **Fig. S1(c)**, ChCl and TCA exhibit characteristic − OH and − CO stretching vibrations around 3330 cm^{-1} and 1720 cm^{-1}, respectively. In the DES (ChCl:TCA), these peaks shift slightly, which indicates the formation of new hydrogen bonds between ChCl and TCA, altering the internal bonding structure of the components. Overall, the shifts in the − OH and − CO stretching frequencies across the DES spectra compared to individual components, suggest the formation of robust hydrogen bond networks, which are likely responsible for the unique physicochemical properties of the DESs.

3.2. Rheological behaviour of DESs

The rheological properties of DESs are crucial in metal recovery processes as they may influence the fluid's flow behaviour, mixing efficiency, and mass transfer rates, all of which impact the effectiveness of metal dissolution and extraction. Higher viscosities can limit diffusion rates, while optimal flow properties enable better contact between DES and metal surfaces, enhancing recovery efficiency. Therefore, the rheological properties of the synthesised DESs were determined using a rheometer in shear mode as described previously. As displayed in Fig. 3, the ChCl:CAA, ChCl:DCA, and ChCl:TCA DESs demonstrated Newtonian behaviour, with viscosity remaining constant regardless of the applied shear rate and time. This behaviour suggests a lack of molecular structuring or entanglements in these DESs [35,36]. Specifically, ChCl:CAA, ChCl:DCA, and ChCl:TCA DESs exhibited stable viscosities of 276.60 mPa.s, 347.84 mPa.s, and 1113.8 mPa.s, respectively. The viscosity values increased with the inclusion of more complex or bulky carboxylic acid components, likely due to stronger hydrogen bonding networks between choline chloride and the acid molecules. This network formation may restrict molecular mobility, resulting in higher viscosities for DESs with bulkier acids like DCA and TCA compared to CAA. In other words, the increasing viscosity from ChCl:CAA DES to ChCl:TCA DES can be attributed to the increasing molecular size, weight, polarity, and strength of intermolecular interactions (especially hydrogen bonding and dipole–dipole interactions) as the number of chlorine atoms of DES HBD increases. This results in a more viscous solvent as the chlorination level of the acid increases.

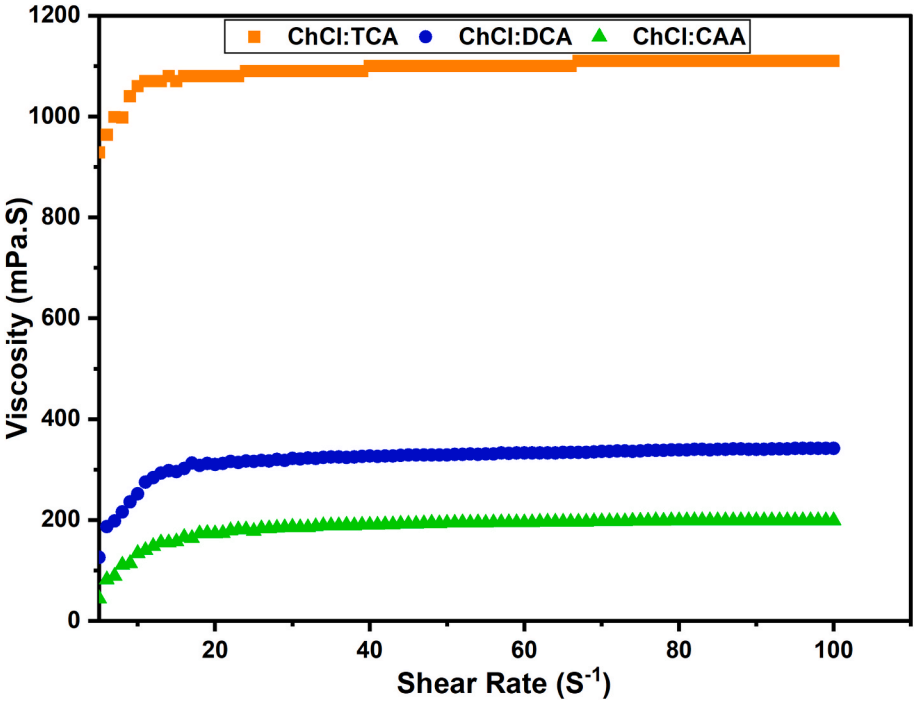

Fig. 3. Flow behaviour of the DESs prepared.

3.3. Roles of various factors on leaching efficiency of DESs

This section discusses the role of key operating parameters in optimising the leaching of base metals (Cu, Al, Fe, Sn and Sc) from WPCBs using carboxylic acid-based DESs. Understanding these factors is essential for enhancing metal recovery in an eco-friendly manner. The nature of the DES is crucial, as its composition influences its interaction with target metals. The grain size of PCB material impacts leaching efficiency, with smaller particles offering more surface area for metal dissolution. In addition, contact time also affects extraction rates, as sufficient interaction time is necessary for optimal metal recovery, though longer times may not always improve efficiency. Temperature generally enhances reaction rates, but excessive heat can degrade the DES, so careful control would be needed. Furthermore, water addition reduces DES viscosity, improving metal solubility, but too much can weaken the DES structure. In addition, the concentration of H_2O_2 as an oxidant boosts metal solubility by increasing oxidation states. Finally, increased agitation improves the leaching efficiency of metals by enhancing the contact between the solvent and the metal surface, thereby facilitating faster and more effective metal dissolution. These

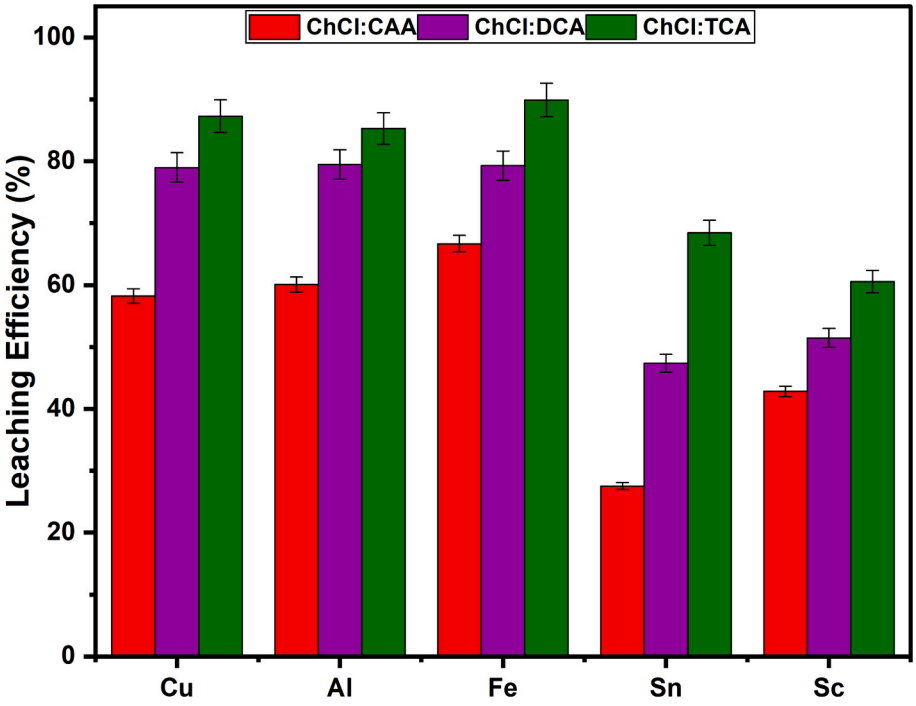

Fig. 4. Role of DES nature on the leaching efficiency of base metals (T = 45 °C; t = 3.0 h; H_2O_2 = 1.0 M; grain size = 212 μm; rpm = 500 & S/L = 1/10).

parameters collectively influence the efficiency, and sustainability of metal recovery in DES-based leaching, highlighting the need for precise optimisation.

3.3.1. DESs nature

In this study, the DESs ChCl:CAA, ChCl:DCA, and ChCl:TCA, each containing chloroacetic, dichloroacetic, or trichloroacetic acid as the hydrogen bond donor were used to leach Cu, Al, Fe, Sn, and Sc from 212 μm grain size of WPCBs. The acidity of each DES, influenced by the pKa of its acid component, affected its metal leaching efficiency. A lower pKa indicates a stronger acid that releases more protons, enhancing the DES's ability to dissolve metals. In contrast, a higher pKa corresponds to weaker acidity and reduced effectiveness in metal recovery[37,38]. This variation in acid strength thus impacted each DES's leaching performance.

As depicted in **Table S2 and** Fig. 4, the leaching efficiency of various metals from WPCBs is influenced by the acidic strength of the DES used. The acidity of each DES can be understood in terms of the pKa values of the HBDs: CAA (pKa = 2.87), DCA (pKa = 1.29), and TCA (pKa = 0.66) [39]. Lower pKa values indicate stronger acids, which dissociate more readily and increase the availability of protons (H^+) in solution, enhancing the DES's capacity to interact with and dissolve metals. In this study, the DES with the lowest pKa, ChCl:TCA, demonstrated the highest leaching efficiencies, achieving leaching efficiencies of 87.3 % for Cu, 85.3 % for Al, 89.9 % for Fe, 68.4 % for Sn, and 60.6 % for Sc. This is in contrast to ChCl:CAA, which, with a higher pKa of 2.87, showed lower leaching efficiencies—58.2 % for Cu, 60.1 % for Al, 66.7 % for Fe, 27.5 % for Sn, and 42.8 % for Sc. ChCl:DCA, with a pKa of 1.29, achieved intermediate leaching efficiencies, reflecting a trend where leaching efficiency improves as acidity increases. The presence of chlorine atoms in the HBDs also plays a key role in enhancing the DES's acidity. As we move from CAA with one chlorine atom, to DCA with two chlorine atoms, and finally to TCA with three chlorine atoms, the acidity strengthens. Chlorine atoms are highly electronegative, drawing electron density away from the carboxyl group, which increases the acid's ability to release protons and thus lowers its pKa. This electronegativity effect contributes to the observed trend in metal leaching: ChCl:TCA, with the highest number of chlorine atoms, has the strongest acidic character and achieves the highest recovery rates, making it the most effective DES for metal leaching among those studied. In other words, the superior performance of ChCl:TCA among the studied DESs is primarily attributed to its enhanced acidity, which is influenced by the number of chlorine atoms in the hydrogen bond donor (HBD). Moving from CAA (one Cl) to DCA (two Cl), and finally to TCA (three Cl), the increasing electronegativity from additional chlorine atoms withdraws electron density from the carboxyl group, thereby lowering the pKa and strengthening the acid. This increased acidity facilitates more effective protonation and metal dissolution. Thus, ChCl:TCA, with the highest number of chlorine atoms, exhibits the strongest acidic character and consequently the highest metal leaching efficiency. Based on this performance, it was selected for further experiments.

3.3.2. Grain size

The influence of grain size on the leaching of the examined metals was assessed using five different grain size fractions: 106, 212, 300, 400, and 500 μm (Fig. 1). As shown in **Table S3 and** Fig. 5, decreasing the grain size enhanced the leaching efficiency of the metals under investigation. After 3 h of leaching with the smallest grain size of 106 μm, the highest efficiencies were observed for Cu (93.4 %), Al (89.2 %), Fe (95.5 %), Sn (72.6 %), and Sc (68.0 %). In contrast, larger grain sizes between 212 and 500 μm showed reduced leaching efficiencies for all investigated metals. This trend can be attributed to the unique characteristics of smaller grains, which enhance the leaching process in several ways: Smaller grains increase the total surface area exposed to the leaching agent, facilitating greater interaction. Additionally, the diffusion pathway for the leaching agent is shorter in smaller grains, allowing it to reach the core more quickly. Finally, finer grains often exhibit higher chemical reactivity due to a greater number of active sites on their surface. These findings align with previously reported results on the influence of grain size on metal leaching efficiency from WPCBs [12,40,41].

3.3.3. Time

The leaching experiment using ChCl:TCA DES reveals that extended

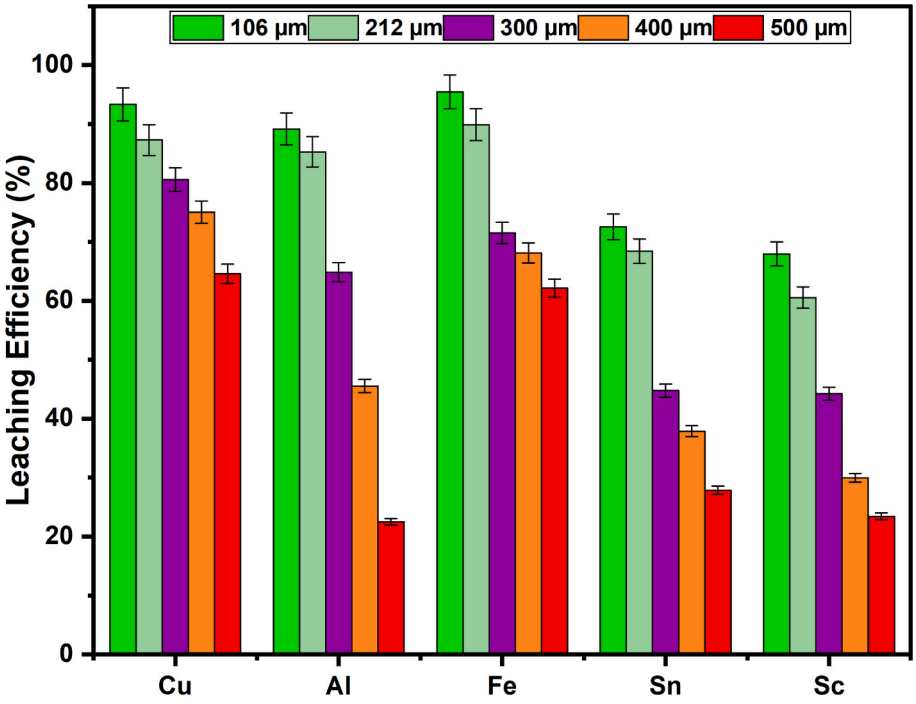

Fig. 5. Role of different grain sizes of WPCBs on the leaching efficiency of base metals (T = 45 °C; t = 3.0 h; H_2O_2 = 1.0 M; grain sizes = 106 − 500 μm; rpm = 500 & S/L = 1/10).

contact times between the DES and WPCBs generally improve metal recovery due to enhanced desorption, diffusion, and complexation processes (**Table S4 and** Fig. 6). In this study, time was varied from 1 h to 5 h at 45 °C and 500 rpm. Cu demonstrated a rapid increase in leaching efficiency from 81.1 % at 1 h to a peak of 99.2 % at 5 h, indicating near-complete leaching. Fe achieved 72.7 % efficiency at 1 h and reached a full 100.0 % leaching by 5 h, underscoring the solvent's efficacy in extracting Fe with minimal time. Al, on the other hand, exhibited a more gradual increase in recovery, rising from 51.7 % at 1 h to 99.8 % at 5 h, showing the advantage of longer contact times for substantial Al leaching. In addition, for Sn, the leaching efficiency improved from 55.4 % at 1 h to 91.7 % at 5 h, with notable increments at 72.6 % (2 h) and 82.3 % (4 h), indicating that extended solvent exposure enhances Sn extraction. Furthermore, Sc presented the lowest initial efficiency, starting at 33.8 % at 1 h and increasing to 79.4 % by 5 h, demonstrating a steady improvement with prolonged contact time. These results suggest that increasing the DES-PCB contact time enables more thorough leaching, especially for metals like Al, Sn, and Sc, which benefit from prolonged interaction for higher leaching efficiencies, while Fe and Cu reach near-complete recovery in a shorter time frame. This highlights the importance of optimising contact time to achieve maximal extraction of metals from PCBs, especially for elements requiring extended diffusion and complexation durations.

3.3.4. Temperature

The rate of chemical reactions is significantly influenced by temperature. A higher temperature causes more molecules to become activated, encourages efficient collisions, and quickens the rate of reaction [12,42]. Fig. 7 illustrates the role of temperature on the leaching efficiency of various metals studied in the temperature range of 25 °C to 65 °C. For Cu, the leaching efficiency increases from 82.9 % at 25 °C to complete recovery (100 % at 65 °C), indicating that higher temperatures enhance Cu. Al shows a similar trend, with an increase from 52.9 % at 25 °C to 98.5 % at 65 °C. On the other hand, Fe reaches maximum efficiency of 100.0 % at 55 °C after rising from 64.0 % at 25 °C, showing that Fe leaching benefits considerably from elevated temperatures. Furthermore, Sn also demonstrates temperature dependence, with leaching efficiency improving from 48.6 % at 25 °C to 91.9 % at 65 °C, reflecting a steady increase across the range. Sc, however, presents a more moderate trend, starting from 34.2 % at 25 °C and reaching 82.6 % at 65 °C, indicating that higher temperatures moderately improve Sc leaching efficiency (**Table S5**). Overall, increasing temperature enhances the leaching efficiencies for all metals, with Fe, Cu, and Al achieving near-complete recovery at higher temperatures.

3.3.5. H_2O_2 concentrations

Fig. 8 demonstrates the influence of varying H_2O_2 concentrations (0 M to 2 M) on the leaching efficiency of the investigated metals. For Cu, the leaching efficiency increases from 78.7 % without H_2O_2 to 99.9 % at 1.5 M, suggesting that higher H_2O_2 concentrations effectively enhance Cu leaching. However, a slight decline in the leaching efficiency of Cu was observed when H_2O_2 was increased to 2 M (98.9 %). Similarly, Al shows a marked increase, with efficiency rising from 42.9 % at 0 M to 97.6 % at 2 M. In addition, Fe also achieves significant leaching efficiency, starting from 67.1 % without H_2O_2 and reaching a complete extraction of 100.0 % at 1.5 M, then slightly declining at 2 M. Furthermore. Sn displays a rapid increase from 32.8 % at 0 M to 86.9 % at 2 M, indicating that higher H_2O_2 concentrations progressively enhance its leaching efficiency. Finally, Sc efficiency improves from 25.5 % at 0 M to 81.6 % at 2 M, showing that although Sc leaching benefits from higher H_2O_2 levels, the improvement is less pronounced than for other metals (**Table S7)**. Overall, the addition of H_2O_2 significantly boosts leaching efficiencies across all metals, particularly for Cu, Al, and Fe, where optimal recovery is achieved at 1.5 M and 2 M H_2O_2. This effect is likely due to the strong oxidising properties of H_2O_2, facilitating metal dissolution and enhancing the efficiency of the DES system. The leaching of metals depends on the presence of O_2 in the acidic system. The leaching system can effectively obtain dissolved O_2 from H_2O_2 due to its potent oxidising properties [43]. According to equations (**2–4**), dissolved O_2 is produced when H_2O_2 breaks down [44]. By reacting with metals, this dissolved O_2 creates metal oxides, which then react with the DES to form the metal-DES complex. A high standard reduction potential of 2.38 V is induced by the OH^- radicals in the leaching solution, aiding in the metals' leaching [26].

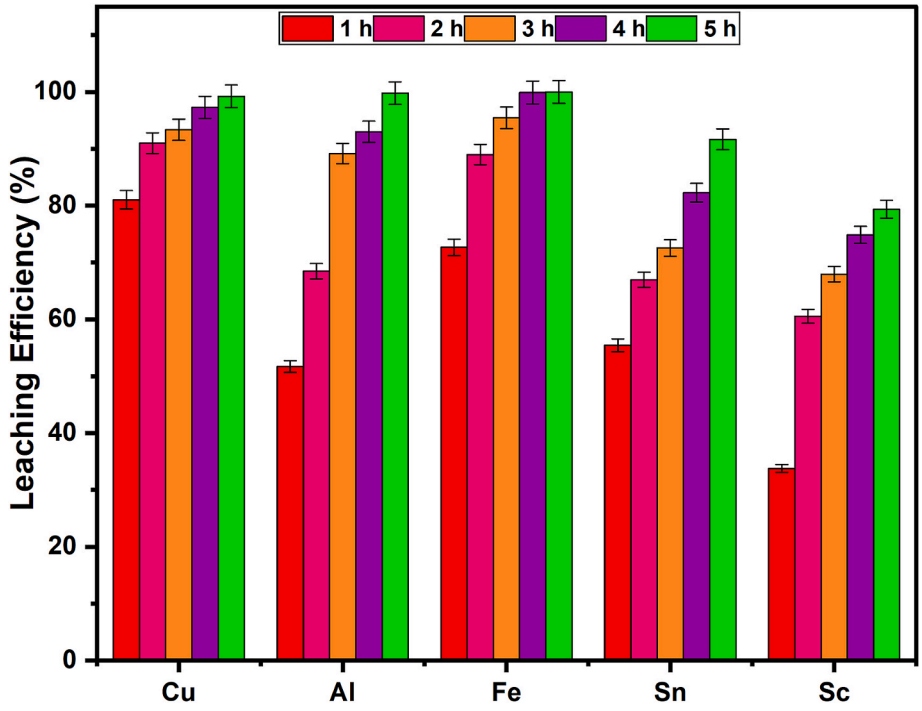

Fig. 6. Role of time on the leaching efficiency of base metals from WPCBs (T = 45 °C; t = 1 – 5h; H_2O_2 = 1.0 M; grain size = 106 μm; rpm = 500 & S/L = 1/10).

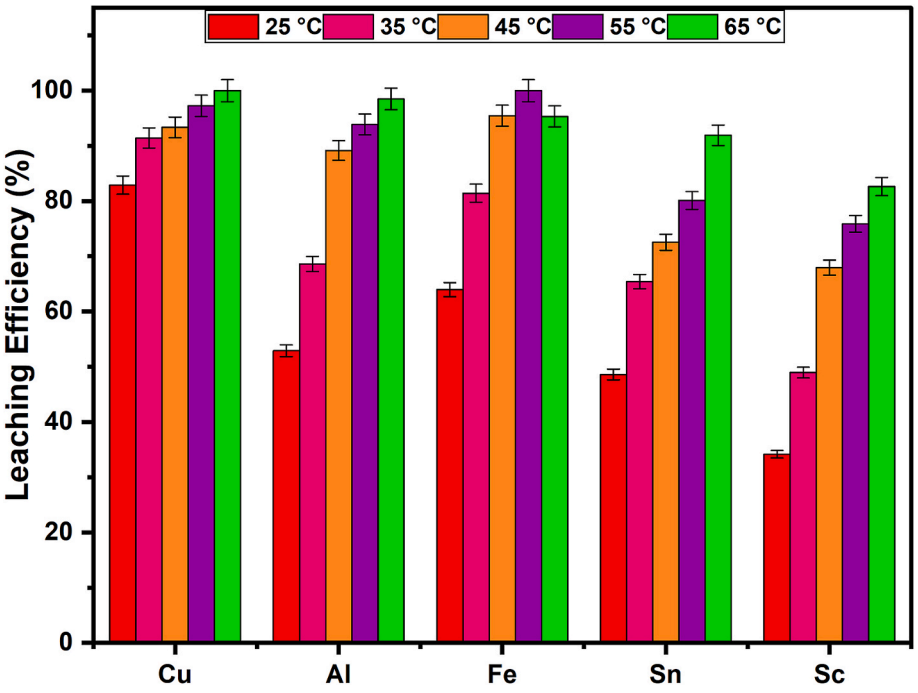

Fig. 7. Role of temperature on the leaching efficiency of base metals from WPCBs (T = 25 − 65 °C; t = 3h; H_2O_2 = 1.0 M; grain size = 106 μm; rpm = 500 & S/L = 1/10).

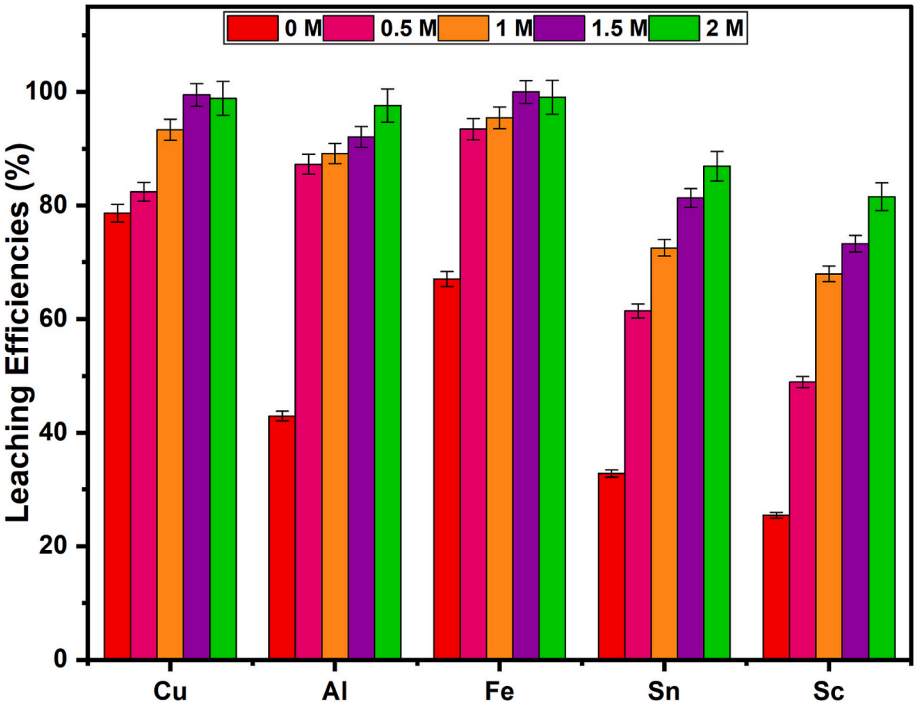

Fig. 8. Role of different concentrations of H_2O_2 on the leaching efficiency of base metals from WPCBs (T = 45 °C; t = 3h; H_2O_2 = 0 − 2 M; grain size = 106 μm; rpm = 500 & S/L = 1/10).

$$H_2O_{2(aq)} + 2e^- \rightarrow 2OH^-_{(aq)} \quad (2)$$

$$H_2O_{2(aq)} + 2e^- \rightarrow OH^-_{(aq)} + OH^-_{(aq)} \quad (3)$$

$$2H_2O_{2(aq)} \rightarrow 2H_2O_{(l)} + O_{2(g)} \quad (4)$$

3.3.6. Agitation speed

Fig. 9 shows the impact of agitation speed on the leaching efficiency of various metals from waste, highlighting that increasing the stirring speed enhances extraction rates significantly. For Cu, leaching efficiency rises from 78.9 % at 300 rpm to a peak of 99.8 % at 700 rpm, with marked increments at each interval. Similarly, Al shows a substantial increase, improving from 56.3 % at 300 rpm to 92.5 % at 700 rpm. Furthermore, Fe benefits as well, reaching its maximum efficiency at

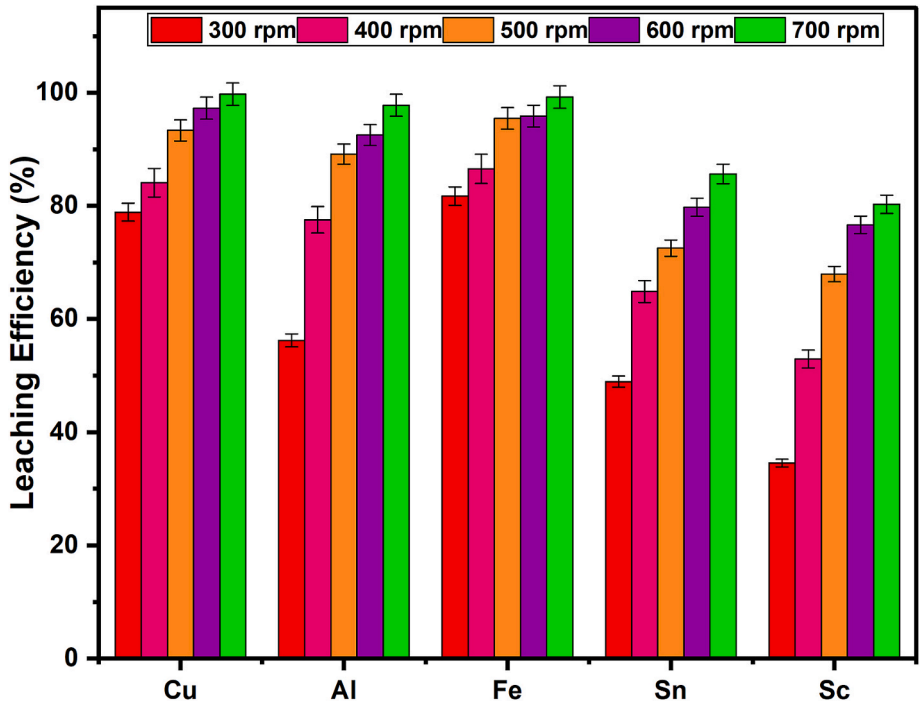

Fig. 9. Role of agitation speed on the leaching efficiency of base metals from WPCBs (T = 45 °C; t = 3h; H_2O_2 = 1 M; grain size = 106 μm; rpm = 300 − 700 & S/L = 1/10).

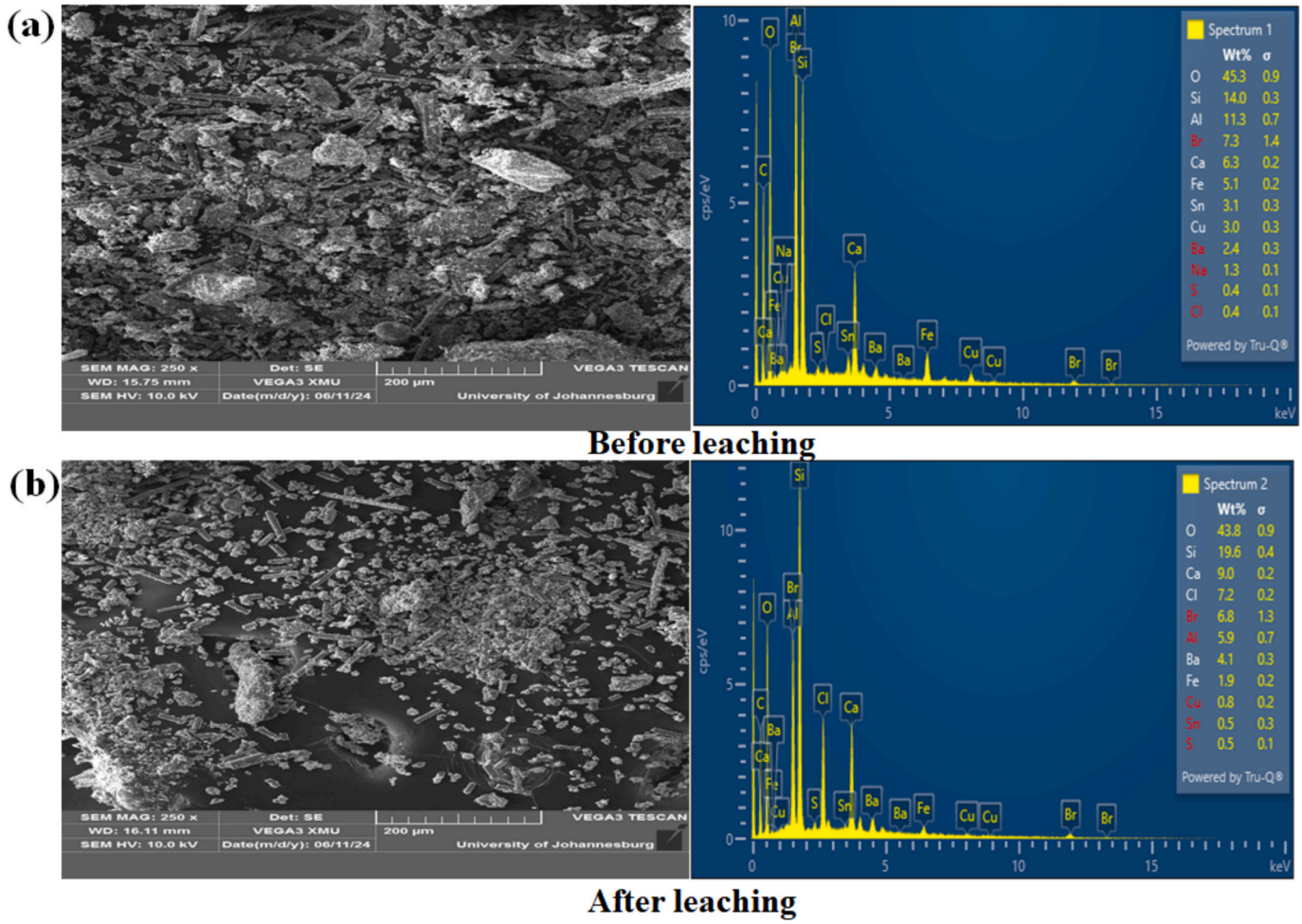

Fig. 10. SEM-EDX of the WPCBs (a) before and (b) after the leaching process.

700 rpm with a leaching efficiency of 99.3 %, up from 81.7 % at 300 rpm. Also, Sn shows a strong response to increased agitation, rising from 49.0 % at 300 rpm to 85.7 % at 700 rpm, while Sc follows a similar trend, with efficiency increasing from 34.5 % at 300 rpm to 80.3 % at 700 rpm (**Table S7**). These results suggest that higher stirring speeds improve the mixing of reactants and enhance mass transfer, facilitating greater diffusion of leaching agents (ChCl:TCA DES + H_2O_2) to the metal surfaces, thus optimising metal extraction [45].

3.4. Analyses of the WPCBs before and after leaching

The combined SEM-EDX and XRD analyses presented in Fig. 10 (**a & b**) and **11** provide a comprehensive view of the structural and compositional changes in the WPCBs before and after leaching with the ChCl:TCA (T = 65 °C; t = 3h; H_2O_2 = 1.0 M; grain size = 106 μm; rpm = 500 & S/L = 1/10). As depicted in Fig. 10**a**, before leaching, the SEM image shows a densely packed, irregular structure with minimal visible porosity, indicating the presence of intact metal particles and complex metal oxide formations within the sample. The surface appears coarse and compact, suggesting a low degree of particle separation or fragmentation. After leaching (Fig. 10**b**), the SEM reveals a more fragmented and porous structure with apparent surface irregularities and voids, indicative of material dissolution. This increased porosity and roughness imply the successful removal of certain metal components, facilitating exposure of inner matrix regions and indicating a level of structural degradation due to leaching. In addition, the EDX data show notable changes in elemental composition. Initially, the unleached WPCB sample contained 3.0 % Cu, 5.1 % Fe, 3.1 % Sn, and 11.3 % Al (by weight), with a mix of other elements such as Si, Ca, Cl, Ba, Br, S and Na (Fig. 10**a**). After leaching, the concentrations of Cu (0.8 %), Fe (1.9 %), Sn (0.5 %) and Al (5.9 %) are drastically reduced in the leached WPCBs (Fig. 10**b**). However, Sc, though targeted, was not detected by EDX, potentially due to its low concentration in the WPCBs.

The XRD analysis of the waste printed circuit boards (WPCBs) before and after treatment with the ChCl:TCA provides clear evidence of phase transformations and metal dissolution. Prior to leaching, the XRD pattern of the untreated WPCBs (Fig. 11) displays sharp, well-defined peaks at 2θ values corresponding to metallic Cu, Al, Fe, and Sn. These peaks are indicative of crystalline phases and align with the following reference standards: Cu (PDF 01–085-1326), Al (PDF 01–089-2769), Fe (PDF 03–065-4899), and Sn (PDF 03–065-0296). Specifically, Cu is identified by characteristic reflections at approximately 43.3°, 50.5°, and 74.1°, attributed to the (111), (200), and (220) planes, respectively. Al is confirmed by peaks at 38.5°, 44.7°, and 65.1°, matching the (111), (200), and (220) planes. Fe is observed at around 44.6°, 65.0°, and 82.3°, corresponding to the (011), (002), and (112) planes. Sn exhibits prominent peaks at 30.6°, 32.0°, 44.9°, and 55.3°, which correlate with the (200), (101), (112), and (103) planes. These findings are consistent with the SEM-EDX results (Fig. 10**a&b**), which confirmed the elemental presence of these metals. Moreover, the compact and dense morphology observed in the SEM image prior to leaching further supports the presence of a predominantly crystalline metallic structure. Following leaching with the ChCl:TCA DES, the XRD pattern shows substantial reductions in peak intensities (Fig. 11). The peaks corresponding to Cu, Fe and Al are no longer detectable or significantly reduced, suggesting their complete dissolution. Al peaks are significantly diminished, particularly at ~ 38.5° and 65.5°, indicating partial leaching with residual traces of Al possibly remaining. In contrast, the Sn peaks remain relatively intense, with all four major reflections (30.6°, 32.0°, 44.9°, and 55.3°) still visible, indicating that Sn was not fully leached under the experimental conditions applied. The overall reduction in peak intensities across the XRD spectrum post-leaching also implies a decrease in the crystalline order, suggesting the transformation of some metallic constituents into amorphous or oxidised forms. This interpretation is supported by the observed increase in oxygen content in the SEM-EDX analysis after leaching, which may reflect the presence of metal oxides or oxygenated residues. In summary, the combined XRD and SEM-EDX results demonstrate the effectiveness of the ChCl:TCA DES in selectively leaching Cu, Fe, and a substantial portion of Al from the WPCBs. However, the persistence of Sn indicates the need for either more aggressive conditions or alternative leaching strategies to achieve complete metal leaching.

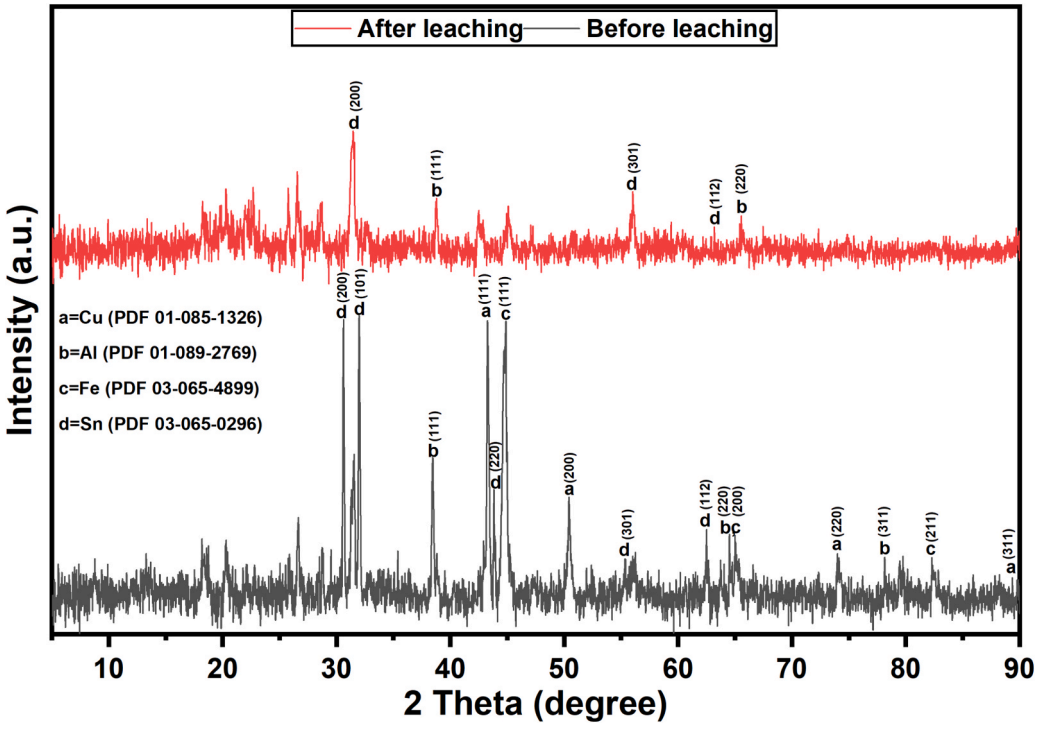

Fig. 11. XRD patterns of the WPCBs before and after the leaching process.

3.5. Leaching mechanism of DES using FT-IR

The FT-IR spectra of the ChCl:TCA DES and the corresponding leachate after leaching (Fig. 12) provide insight into the leaching mechanism under the experimental conditions: temperature of 65 °C, time of 3 h, H_2O_2 concentration of 1.0 M, particle size of 106 μm, stirring speed of 500 rpm, and S/L of 1/10. In the original ChCl:TCA DES FT-IR spectra, the broad absorption bands around 3322 cm^{-1} and 2975 cm^{-1} correspond to O–H and C–H stretching vibrations, respectively, which are characteristic of hydrogen-bonding interactions within the DES matrix. Additionally, a notable peak at 1755 cm^{-1} represents the C=O stretching vibration from the TCA component in the DES. The presence of peaks around 1473 cm^{-1} and 1392 cm^{-1} are attributed to the bending vibrations of the C–H bonds, while the absorption at 1208 cm^{-1} corresponds to C–N stretching, indicative of the ChCl structure. The peak around 953 cm^{-1} could be attributed to C–Cl stretching, which reflects the presence of Cl in the DES.

In the FT-IR spectra of the leachate, several significant shifts and changes are observed, reflecting interactions between the DES and the WPCB materials. The broad O–H stretching band shifts slightly to a higher frequency at 3371 cm^{-1}, and a new peak (C–H stretching) appears at 2986 cm^{-1}, indicating possible changes in the hydrogen-bonding environment and suggesting that metal ion complexation may have occurred. The C=O stretching peak shifts from 1755 cm^{-1} in the DES to 1750 cm^{-1} in the leachate, with a reduction in intensity. This shift implies that the C=O in the DES have engaged in complexation with metal ions released from the WPCBs, supporting their role as ligands in metal coordination [46]. Additional peaks in the leachate around 1660 cm^{-1} and 1478 cm^{-1} indicate the formation of new compounds, potentially from metal complexes or oxidation products of organic components in the DES. The appearance of these new peaks, along with the altered C–Cl stretching around 955 cm^{-1} and the O–H bending at 446 cm^{-1}, reinforces the idea of chemical transformations and interactions between the DES components and the leached metals.

The spectra changes observed in the FT-IR data suggest that the ChCl:TCA DES facilitates metal ion release from the WPCBs through a combination of acid dissolution and complexation. The hydrogen bonding and C=O functional groups in the DES likely play essential roles in coordinating with metal ions, enabling their extraction from the solid matrix of the WPCBs [47]. In summary, the FT-IR analysis indicates that the ChCl:TCA DES engages in hydrogen bonding and complexation interactions, leading to the dissolution and removal of metals from the WPCBs. The shift and intensity changes of key functional groups, such as O–H and C=O, after leaching, highlight the DES's capability to complex with and extract metal ions, thereby supporting the proposed leaching mechanism.

3.6. Leaching kinetics

Examining the leaching curves and kinetics of metals over a range of temperatures (from 25 °C to 65 °C) and durations (0.5 h to 3 h) provided insight into the leaching mechanism of metals from WPCBs in ChCl:TCA DES. Understanding the leaching kinetics is essential for investigating how metals dissolve from the separated metallic layers of WPCBs. To analyse the reaction kinetics in this context, the widely used shrinking core model (SCM) was employed. In solid–liquid reaction systems like this, the leaching process is typically governed either by diffusion through a product layer or by chemical reactions occurring at the surface using equations (5) and (6), respectively [48].

$$k_a t = 1 - 3(1 - X)^{2/3} + 2(1 - X) \quad (5)$$

$$k_b t = 1 - (1 - X)^{1/3} \quad (6)$$

In this case, k_a and k_b denote the kinetic rate constants for the diffusion-controlled and chemical reaction-controlled reactions, respectively (min^{-1}), t represents reaction time (min) and X designates the leaching fraction.

When the aforementioned kinetic equations were applied to the experimental data, the leaching of all metals under study using both the diffusion and chemical reaction-controlled models showed a good and nearly identical linear fitting. These R^2 values show that there is no obvious difference between the diffusion-controlled model (**Fig. S2**) and

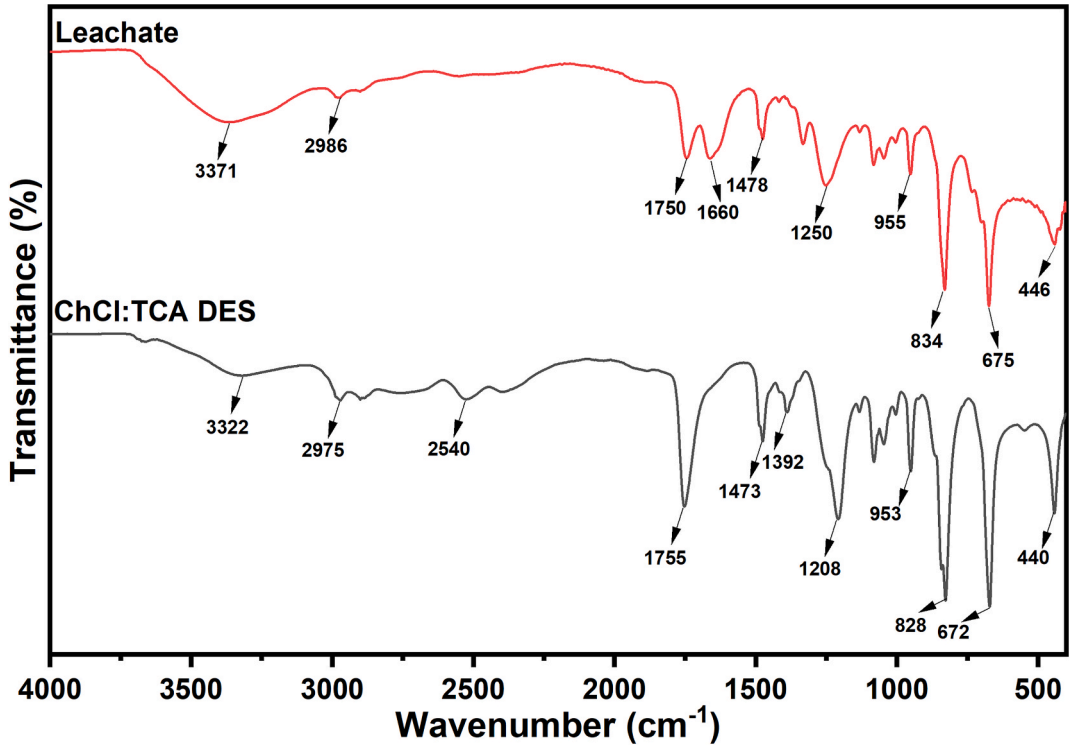

Fig. 12. FT-IR spectra of ChCl:TCA DES and its leachate.

the chemical reaction-controlled model (**Fig. S3**). Both kinetic models showed R^2 values that are close to 1 in most cases. In order to further evaluate the kinetic model of the leaching process, a range of experimental activation energies is computed using the Arrhenius plots. The values of k_a and k_b were taken from the slopes of the linear plots (**Fig. S2 & S3**) and applied to the Arrhenius equation to determine the experimental activation energy (Ea).

$$k = Ae^{-Ea/RT} \tag{7}$$

where k denotes the rate constant, A represents the frequency factor, Ea designates the activation energy, or the energy threshold for the reaction to proceed, R depicts the universal gas constant (8.314 J/mol/K), T symbolises the temperature of the reaction in Kelvin.

Using the diffusion-controlled model's k values to estimate activation energies with the Arrhenius equation, we obtained 9.2 $kJmol^{-1}$, 34.0 $kJmol^{-1}$, 31.0 $kJmol^{-1}$, 29.5 $kJmol^{-1}$, and 23.4 $kJmol^{-1}$ for the leaching of Cu, Al, Fe, Sn, and Sc, respectively, from WPCBs with the ChCl:TCA DES (Fig. 13). Additionally, when applying the k values from the chemical reaction-controlled model, the calculated activation energies for the leaching of Cu, Al, Fe, Sn, and Sc were 18.7 $kJmol^{-1}$, 20.5 $kJmol^{-1}$, 23.9 $kJmol^{-1}$, 11.2 $kJmol^{-1}$, and 25.1 $kJmol^{-1}$, respectively (**Fig. S4**). Literature indicates that apparent activation energies below 40 $kJmol^{-1}$ generally imply a diffusion-controlled process, whereas values over 40 $kJmol^{-1}$ are characteristic of a rate-determining step controlled by chemical reactions [38,49–51]. The leaching of the metals using ChCl:TCA DES is majorly diffusion-controlled, as all of the activation energies for the metals under investigation in our study fall below the 40 kJ/mol threshold. This suggests that rather than the inherent chemical reactions at the solid–liquid interface, the transport of metal ions within the DES matrix may have a greater impact on the overall recovery process. As demonstrated by our findings, diffusion-controlled processes frequently result in increased reaction rates at moderate temperatures. Because it supports the possibility of effective metal recovery under comparatively mild conditions without requiring high energy inputs, this result is beneficial for real-world applications.

4. Conclusions

The findings of this study demonstrate the effectiveness of using carboxylic acid-based DESs for the leaching of base metals, including Cu, Al, Fe, Sn, and Sc from WPCBs. Our comprehensive investigation of key parameters revealed that optimised leaching conditions, including time, temperature, H_2O_2 concentration, and agitation speed, significantly enhance metal leaching. The ChCl:TCA DES (although it has the highest viscosity) outperformed other DESs (ChCl:CAA and ChCl:CAA) due to its stronger hydrogen bonding network and acidic character, achieving near-complete leaching efficiency for Cu, Al, Fe, Sn, and Sc under mild conditions. Characterisation techniques confirmed substantial structural changes post-leaching, with SEM-EDX and XRD analyses showing significant metal removal and increased porosity. FT-IR spectra further indicated complexation and interaction between DES components and metal ions, supporting the DES's role in metal dissolution. The kinetic analysis, with activation energies below 40 $kJmol^{-1}$ for all metals investigated confirms a diffusion-controlled process, which aligns with the potential for efficient metal leaching at moderate temperatures. These results suggest that ChCl:TCA DES is highly suitable for sustainable e-waste recycling. Overall, this study contributes a novel, eco-friendly approach to e-waste recycling that aligns with sustainability goals by reducing the environmental impact of traditional methods. Our findings support the use of DESs as viable alternatives for WPCB recycling, offering economic feasibility for real-world applications in metal recovery. While this study demonstrated the high efficiency of metal leaching from WPCBs using carboxylic acid-based DESs, the separation and recovery of individual metals remain essential for full process development and will be addressed in future work. This study establishes a critical first step toward full recycling by demonstrating the feasibility of effective metal extraction, upon which downstream recovery and purification strategies can be developed. We also attempted preliminary methods for DES recovery; however, the heterogeneous nature of the WPCBs presented significant challenges. In addition, we intend to add about 40 wt% water to the DES in order to ensure a more sustainable approach if DES regeneration proves abortive in the future. Research has shown that water up to 42 wt% could be added to DES without destroying its hydrogen bonding network [52]. Therefore, future investigations will focus on optimising metal separation routes, improving DES recyclability, and ensuring overall process sustainability. Additionally, planned techno-economic analysis (TEA) and life cycle assessment (LCA) studies will provide a comprehensive evaluation of the feasibility and environmental impact of the proposed approach.

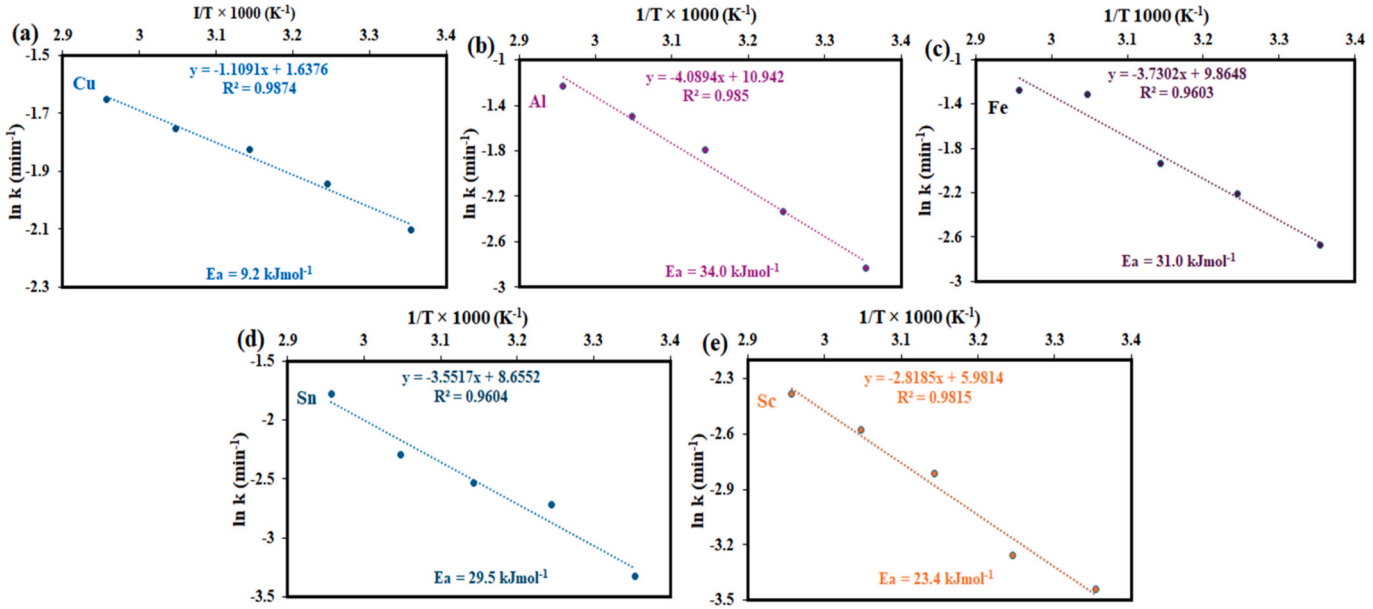

Fig. 13. (a-e). Arrhenius plots for diffusion-controlled leaching mechanism for (a) Cu (b) Al (c) Fe (d) Sn (e) Sc.

5. Author statement

On behalf of all my co-author, I, Emmanuel Oke confirmed that the manuscript is original and not be published in elsewhere.

CRediT authorship contribution statement

Emmanuel Anuoluwapo Oke: Project administration, Formal analysis, Investigation, Conceptualization, Software, Methodology, Data curation, Writing – original draft, Writing – review & editing, Funding acquisition. **Johannes Hermanus Potgieter:** Conceptualization, Resources, Writing – review & editing, Supervision, Funding acquisition.

Funding

E.A. Oke acknowledges the generous financial support provided by the Oppenheimer Memorial Trust (OMT Ref. 2024-4758).

Declaration of competing interest

The authors declare that they have no known competing financial interests or personal relationships that could have appeared to influence the work reported in this paper.

Acknowledgements

We express our appreciation to Mr Bruce Mothibedi for assisting us in sourcing the HP desktop computers' central processing units used for this study. In addition, we extend our gratitude to Dr Joseph Nyembwe for his assistance with the crushing of the printed circuit boards.

Appendix A. Supplementary data

Supplementary data to this article can be found online at https://doi.org/10.1016/j.seppur.2025.133712.

Data availability

Data will be made available on request.

References

[1] R. Rajesh, D. Kanakadhurga, N. Prabaharan, Electronic waste: a critical assessment on the unimaginable growing pollutant, legislations and environmental impacts, Environ. Challenges 7 (2022) 100507, https://doi.org/10.1016/j.envc.2022.100507.
[2] X. Zhu, C. Nie, H. Zhang, X. Lyu, Y. Tao, J. Qiu, L. Li, G. Zhang, Recovery of high-grade copper from waste printed circuit boards by mechanical-grinding assisted flotation, J. Clean. Prod. 232 (2019) 1251–1256, https://doi.org/10.1016/j.jclepro.2019.06.063.
[3] C. Nie, X. Li, Q. Sun, Q. Gao, X. Zhu, X. Lyu, L. Li, X. You, Clean and efficient process for the recycling of all components from waste printed circuit boards: pre-treatment, bio-metallurgy, and deep utilization, J. Clean. Prod. 466 (2024) 142810, https://doi.org/10.1016/j.jclepro.2024.142810.
[4] C.P. Baldé, R. Kuehr, T. Yamamoto, R. McDonald, S. Althaf, G. Bel, O. Deubzer, E. Fernandez-Cubillo, V. Forti, V. Gray, S. Herat, S. Honda, G. Iattoni, D. S. Khetriwal, V. Luda di Cortemiglia, The Global E-Waste Monitor 2024, nternational Telecommunication Union (ITU) and United Nations Institute for Training and Research (UNITAR), Switzerland, Geneva, 2024 https://www.itu.int/itu-d/sites/environment.
[5] X. Zhu, C. Nie, S. Wang, Y. Xie, H. Zhang, X. Lyu, J. Qiu, L. Li, Cleaner approach to the recycling of metals in waste printed circuit boards by magnetic and gravity separation, J. Clean. Prod. 248 (2020) 119235, https://doi.org/10.1016/j.jclepro.2019.119235.
[6] U. Domańska, A. Wiśniewska, Z. Dąbrowski, Recovery of strategic metals from waste printed circuit boards with deep eutectic solvents and ionic liquids, Processes 12 (2024) 530, https://doi.org/10.3390/pr12030530.
[7] R. Panda, S. Mishra, K.K. Pant, T. Bhaskar, S.N. Naik, A closed loop recycling strategy for sustainable recovery of group 11 metals (Cu, Au, and Ag) from waste PCBs: an amalgamation of low-temperature NH_4Cl roasting, Hcl Leaching and Cementation, Sustain. Mater. Technol. 37 (2023) e00652, https://doi.org/10.1016/j.susmat.2023.e00652.
[8] V. Beiki, T. Naseri, S.M. Mousavi, Comprehensive characterization and environmental implications of spent telecommunication printed circuit boards: Towards a cleaner and sustainable environment, J. Environ. Manage. 325 (2023) 116482, https://doi.org/10.1016/j.jenvman.2022.116482.
[9] S.S.V. Vuppaladadiyam, B.S. Thomas, C. Kundu, A.K. Vuppaladadiyam, H. Duan, S. Bhattacharya, Can e-waste recycling provide a solution to the scarcity of rare earth metals? An Overview of e-Waste Recycling Methods, Sci. Total Environ. 924 (2024) 171453, https://doi.org/10.1016/j.scitotenv.2024.171453.
[10] T. Watari, K. Nansai, K. Nakajima, Major metals demand, supply, and environmental impacts to 2100: A critical review, Resour. Conserv. Recycl. 164 (2021) 105107, https://doi.org/10.1016/j.resconrec.2020.105107.
[11] B.W. Schipper, H.-C. Lin, M.A. Meloni, K. Wansleeben, R. Heijungs, E. van der Voet, Estimating global copper demand until 2100 with regression and stock dynamics, Resour. Conserv. Recycl. 132 (2018) 28–36, https://doi.org/10.1016/j.resconrec.2018.01.004.
[12] E.A. Oke, H. Potgieter, Recent chemical methods for metals recovery from printed circuit boards: a review, J Mater Cycles Waste Manag 26 (2024) 1349–1368, https://doi.org/10.1007/s10163-024-01944-4.
[13] D. Zou, R. Chen, K. Zhao, X. Wang, X. Huang, Z. Wang, Secondary resource utilization of electronic waste: a review of extraction and recovery of precious metals, Min. Metall. Explor. 41 (2024) 1739–1753, https://doi.org/10.1007/s42461-024-01002-5.
[14] G. Zha, C. Yang, Y. Wang, X. Guo, W. Jiang, B. Yang, New vacuum distillation technology for separating and recovering valuable metals from a high value-added waste, Sep. Purif. Technol. 209 (2019) 863–869, https://doi.org/10.1016/j.seppur.2018.09.038.
[15] Y. Chen, S. Liang, K. Xiao, J. Hu, H. Hou, B. Liu, H. Deng, J. Yang, A cost-effective strategy for metal recovery from waste printed circuit boards via crushing pretreatment combined with pyrolysis: effects of particle size and pyrolysis temperature, J. Clean. Prod. 280 (2021) 124505, https://doi.org/10.1016/j.jclepro.2020.124505.
[16] F. Faraji, R. Golmohammadzadeh, C.A. Pickles, Potential and current practices of recycling waste printed circuit boards: a review of the recent progress in pyrometallurgy, J. Environ. Manage. 316 (2022) 115242, https://doi.org/10.1016/j.jenvman.2022.115242.
[17] P.R. Jadhao, E. Ahmad, K.K. Pant, K.D.P. Nigam, Environmentally friendly approach for the recovery of metallic fraction from waste printed circuit boards using pyrolysis and ultrasonication, Waste Manag. 118 (2020) 150–160, https://doi.org/10.1016/j.wasman.2020.08.028.
[18] P. Kaur, S. Sharma, F.M. Albarakaty, A. Kalia, M.M. Hassan, K.A. Abd-Elsalam, Biosorption and bioleaching of heavy metals from electronic waste varied with microbial genera, Sustainability 14 (2022) 935, https://doi.org/10.3390/su14020935.
[19] J. An, Characteristics of metals leached from waste printed circuit boards using acidithiobacillus ferrooxidans, Minerals 11 (2021) 224, https://doi.org/10.3390/min11020224.
[20] M. Annamalai, K. Gurumurthy, Enhanced bioleaching of copper from circuit boards of computer waste by Acidithiobacillus ferrooxidans, Environ. Chem. Lett. 17 (2019) 1873–1879, https://doi.org/10.1007/s10311-019-00911-y.
[21] N. Iglesias-Gonzalez, P. Ramirez, J. Lorenzo-Tallafigo, A. Romero-García, A. Mazuelos, R. Romero, F. Carranza, Copper recovery from unground printed circuit board by biogenic ferric at high solid/liquid ratio, Miner. Eng. 180 (2022) 107471, https://doi.org/10.1016/j.mineng.2022.107471.
[22] V. Arslan, Bacterial leaching of copper, zinc, nickel and aluminum from discarded printed circuit boards using acidophilic bacteria, J. Mater. Cycles Waste Manag. 23 (2021) 2005–2015, https://doi.org/10.1007/s10163-021-01274-9.
[23] H. Li, J. Eksteen, E. Oraby, Hydrometallurgical recovery of metals from waste printed circuit boards (WPCBs): Current status and perspectives – A review, Resour. Conserv. Recycl. 139 (2018) 122–139, https://doi.org/10.1016/j.resconrec.2018.08.007.
[24] J. Hao, Y. Wang, Y. Wu, F. Guo, Metal recovery from waste printed circuit boards: a review for current status and perspectives, Resour. Conserv. Recycl. 157 (2020), https://doi.org/10.1016/j.resconrec.2020.104787.
[25] R. Seif El-Nasr, S.M. Abdelbasir, A.H. Kamel, S.S.M. Hassan, Environmentally friendly synthesis of copper nanoparticles from waste printed circuit boards, Sep. Purif. Technol. 230 (2020) 115860, https://doi.org/10.1016/j.seppur.2019.115860.
[26] P.R. Jadhao, A. Pandey, K.K. Pant, K.D.P. Nigam, Efficient recovery of Cu and Ni from WPCB via alkali leaching approach, J. Environ. Manage. 296 (2021) 113154, https://doi.org/10.1016/j.jenvman.2021.113154.
[27] Q. Xia, H. Zhang, K. Liu, J. Li, X. Zhang, Y. Xie, T. Qi, Clean recovery of copper from waste printed circuit boards using ceric ammonium nitrate, Sep. Purif. Technol. 324 (2023) 124474, https://doi.org/10.1016/j.seppur.2023.124474.
[28] F. Feng, M. Wang, J. Zhang, H. Ding, L. Yu, W. Guo, L. Guo, Q. Liang, Q. Zhang, C. Lu, X. Li, Hydrogen bonding-based deep eutectic solvents for choline chloride/sulfamide and its application in the recycling of precious metals, J. Environ. Chem. Eng. 12 (2024), https://doi.org/10.1016/j.jece.2024.113611.
[29] A.P. Abbott, D. Boothby, G. Capper, D.L. Davies, R.K. Rasheed, Deep eutectic solvents formed between choline chloride and carboxylic acids: versatile alternatives to ionic liquids, J. Am. Chem. Soc. 126 (2004) 9142–9147, https://doi.org/10.1021/ja048266j.
[30] O. Mokhodoeva, V. Maksimova, A. Shishov, V. Shkinev, Separation of platinum group metals using deep eutectic solvents based on quaternary ammonium salts, Sep. Purif. Technol. 305 (2023) 122427, https://doi.org/10.1016/j.seppur.2022.122427.

[31] E.A. Oke, Examining the effectiveness of deep eutectic solvents in removal of sulfur from fuel oil: a mini review, Chem. Afr. 7 (2024) 3565–3578, https://doi.org/10.1007/s42250-024-00989-0.
[32] E.A. Oke, Sustainable advancements in hazardous gases capture: Harnessing the potential of deep eutectic solvents, Sustain. Chem. Environ. 6 (2024) 100083, https://doi.org/10.1016/j.scenv.2024.100083.
[33] Z. Wang, M.Y.H. Li, Z.-R.-R. Liu, M.-F. Zhou, Scandium: ore deposits, the pivotal role of magmatic enrichment and future exploration, Ore Geol. Rev. 128 (2021) 103906, https://doi.org/10.1016/j.oregeorev.2020.103906.
[34] R.S.B. Ferreira, A.M. Ferreira, J.A.P. Coutinho, E.A.C. Batista, Stability of cholinium chloride-based deep eutectic solvents with carboxylic acids: a study on ester formation, ACS Sustain. Chem. Eng. (2024), https://doi.org/10.1021/acssuschemeng.4c02903.
[35] I.M. Aroso, A. Paiva, R.L. Reis, A.R.C. Duarte, Natural deep eutectic solvents from choline chloride and betaine – physicochemical properties, J. Mol. Liq. 241 (2017) 654–661, https://doi.org/10.1016/j.molliq.2017.06.051.
[36] H. Zhu, S. Chen, T. Yang, X. Hu, W. Cai, X. Wang, J. He, Y. Luo, Comparative efficiency of different polyol-based deep eutectic solvents for chitin extraction from lobster shells, Int. J. Biol. Macromol. 277 (2024) 134425, https://doi.org/10.1016/j.ijbiomac.2024.134425.
[37] N. Kumar, R. Gautam, J.D. Stallings, G.G. Coty, J.G. Lynam, Secondary agriculture residues pretreatment using deep eutectic solvents, Waste Biomass Valoriz. 12 (2021) 2259–2269, https://doi.org/10.1007/s12649-020-01176-1.
[38] E.A. Oke, H. Potgieter, F. Mondlane, N.P. Skosana, S. Teimouri, J.K. Nyembwe, Concurrent leaching of copper and cobalt from a copper–cobalt ore using sulfuric and organic acids, Miner. Eng. 216 (2024) 108853, https://doi.org/10.1016/j.mineng.2024.108853.
[39] David R Lide, CRC Handbook of Chemistry and Physics, 84th Edition Edited by David R. Lide (National Institute of Standards and Technology). CRC Press LLC: Boca Raton. 2003. 2616 pp. $139.95. ISBN 0-8493-0484-9., J. Am. Chem. Soc. 126 (2004) 1586–1586. doi: 10.1021/ja0336372.
[40] D. Zhang, L. Dong, Y. Li, Y. Wu, Y. Ma, B. Yang, Copper leaching from waste printed circuit boards using typical acidic ionic liquids recovery of e-wastes' surplus value, Waste Manag. 78 (2018) 191–197, https://doi.org/10.1016/j.wasman.2018.05.036.
[41] J. Huang, M. Chen, H. Chen, S. Chen, Q. Sun, Leaching behavior of copper from waste printed circuit boards with Brønsted acidic ionic liquid, Waste Manag. 34 (2014) 483–488, https://doi.org/10.1016/j.wasman.2013.10.027.
[42] T. Zhang, J. Dao, J. Wang, R. wan, C. Li, D. Wang, C. Bao, Y. Zhang, Z. Zhang, P. Dong, Efficient leaching of valuable metals from NCM cathode materials by green deep eutectic solvent, J. Clean. Prod. 438 (2024) 140636. doi: 10.1016/j.jclepro.2024.140636.
[43] Z. Wang, S. Guo, C. Ye, Leaching of copper from metal powders mechanically separated from waste printed circuit boards in chloride media using hydrogen peroxide as oxidant, procedia, Environ. Sci. 31 (2016) 917–924, https://doi.org/10.1016/j.proenv.2016.02.110.
[44] H. Li, E. Oraby, J. Eksteen, Extraction of copper and the co-leaching behaviour of other metals from waste printed circuit boards using alkaline glycine solutions, Resour. Conserv. Recycl. 154 (2020) 104624, https://doi.org/10.1016/j.resconrec.2019.104624.
[45] A. Preetam, A. Modak, P.R. Jadhao, S.N. Naik, K.K. Pant, V. Kumar, A comprehensive study on the extraction of transition metals from waste random access memory using acetic acid as a chelating solvent, J. Environ. Chem. Eng. 10 (2022) 108761, https://doi.org/10.1016/j.jece.2022.108761.
[46] S. Zheng, S. Xu, Z. Wang, H. Duan, D. Chen, M. Long, Y. Li, Efficient leaching of valuable metals from spent lithium-ion batteries using green deep eutectic solvents: Process optimization, mechanistic analysis, and environmental impact assessment, J. Clean. Prod. 480 (2024) 144128, https://doi.org/10.1016/j.jclepro.2024.144128.
[47] L. Chen, Y. Chao, X. Li, G. Zhou, Q. Lu, M. Hua, H. Li, X. Ni, P. Wu, W. Zhu, Engineering a tandem leaching system for the highly selective recycling of valuable metals from spent Li-ion batteries, Green Chem. 23 (2021) 2177–2184, https://doi.org/10.1039/D0GC03820B.
[48] M.D. Rao, K.K. Singh, C.A. Morrison, J.B. Love, Optimization of process parameters for the selective leaching of copper, nickel and isolation of gold from obsolete mobile phone PCBs, Clean. Eng. Technol. 4 (2021) 100180, https://doi.org/10.1016/j.clet.2021.100180.
[49] C.L. Aguirre, N. Toro, N. Carvajal, H. Watling, C. Aguirre, Leaching of chalcopyrite (CuFeS2) with an imidazolium-based ionic liquid in the presence of chloride, Miner. Eng. 99 (2016) 60–66, https://doi.org/10.1016/j.mineng.2016.09.016.
[50] F. Faraji, A. Alizadeh, F. Rashchi, N. Mostoufi, Kinetics of leaching: a review, Rev. Chem. Eng. 38 (2022) 113–148, https://doi.org/10.1515/revce-2019-0073.
[51] S. Teimouri, J.H. Potgieter, M. Lundström, C. Billing, B.P. Wilson, A new hydrometallurgical process for metal extraction from electric arc furnace dust using ionic liquids, Materials 15 (2022) 8648, https://doi.org/10.3390/ma15238648.
[52] O.S. Hammond, D.T. Bowron, K.J. Edler, Structure and properties of "Type IV" lanthanide nitrate hydrate:urea deep eutectic solvents, ACS Sustain. Chem. Eng. 7 (2019) 4932–4940, https://doi.org/10.1021/acssuschemeng.8b05548.